Radiotherapy and Oncology 159 (2021) 136–143

Contents lists available at ScienceDirect

Radiotherapy and Oncology

journal homepage: www.thegreenjournal.com

Original Article

Dosimetric influence of deformable image registration uncertainties on propagated structures for online daily adaptive proton therapy of lung cancer patients

Lena Nenoff [a,b,*], Michael Matter [a,b], Enrique Javier Amaya [a], Mirjana Josipovic [c], Antje-Christin Knopf [d], Antony John Lomax [a,b], Gitte F Persson [c,e,f], Cássia O Ribeiro [d], Sabine Visser [d], Marc Walser [a], Damien Charles Weber [a,g,h], Ye Zhang [a], Francesca Albertini [a]

[a] Paul Scherrer Institute, Center for Proton Therapy; [b] Department of Physics, ETH Zurich, Switzerland; [c] Department of Oncology, Rigshospitalet Copenhagen University Hospital, Denmark; [d] Department of Radiation Oncology, University Medical Center Groningen, University of Groningen, The Netherlands; [e] Department of Oncology, Herlev-Gentofte Hospital Copenhagen University Hospital; [f] Department of Clinical Medicine, Faculty of Medical Sciences, University of Copenhagen, Denmark; [g] Department of Radiation Oncology, University Hospital Zurich; and [h] Department of Radiation Oncology, University Hospital Bern, Switzerland

ARTICLE INFO

Article history:
Received 11 November 2020
Received in revised form 14 March 2021
Accepted 15 March 2021
Available online 23 March 2021

Keywords:
Proton therapy
Structure propagation
Online adaption
Lung cancer

ABSTRACT

Purpose: A major burden of introducing an online daily adaptive proton therapy (DAPT) workflow is the time and resources needed to correct the daily propagated contours. In this study, we evaluated the dosimetric impact of neglecting the online correction of the propagated contours in a DAPT workflow.
Material and methods: For five NSCLC patients with nine repeated deep-inspiration breath-hold CTs, proton therapy plans were optimised on the planning CT to deliver 60 Gy-RBE in 30 fractions. All repeated CTs were registered with six different clinically used deformable image registration (DIR) algorithms to the corresponding planning CT. Structures were propagated rigidly and with each DIR algorithm and reference structures were contoured on each repeated CT. DAPT plans were optimised with the uncorrected, propagated structures (*propagated DAPT doses*) and on the reference structures (*ideal DAPT doses*), *non-adapted doses* were recalculated on all repeated CTs.
Results: Due to anatomical changes occurring during the therapy, the clinical target volume (CTV) coverage of the *non-adapted doses* reduces on average by 9.7% (V95) compared to an *ideal DAPT doses*. For the *propagated DAPT doses*, the CTV coverage was always restored (average differences in the CTV V95 < 1% compared to the *ideal DAPT doses*). Hotspots were always reduced with any DAPT approach.
Conclusion: For the patients presented here, a benefit of online DAPT was shown, even if the daily optimisation is based on propagated structures with some residual uncertainties. However, a careful (offline) structure review is necessary and corrections can be included in an offline adaption.

Introduction

Online daily adaptive proton therapy (DAPT), specifically an optimization directly before the delivery of each fraction, allows for fast reactions to anatomical changes during the treatment course. Currently, similar online adaptive radiotherapy workflows are clinically implemented in several centers with MRI-linacs [1,2], MRI-Cobalt machines [3–5] or standard linacs with Cone-beam CTs (e.g. Varian Ethos [6]). One of the main challenges is to define the contours on the daily image. This has to be performed as quickly as possible, while guaranteeing a high accuracy. Typically, daily contours are generated either by propagation of the planning contours [7,8] after having deformed the daily to the planning image, or by automatic segmentation of the daily image [9–11]. The contour propagation process takes in general less than a minute, whereas for an automatic segmentation about 5–10 minutes are necessary [12]. Additionally, after the daily volumes have been generated, medical doctors need typically approximately 15 minutes to inspect and correct contours of the tumour and the organs-at-risk (OARs) in proximity to the target [2,3]. It is recognised, that the availability of daily contours is nowadays the main bottleneck for the widespread use of online adaption.

Non-small cell lung-cancer (NSCLC) tumours are surrounded by dose-sensitive OARs, such as the lung, heart or oesophagus. Therefore, the improved normal tissue sparing offered by proton therapy

* Corresponding author: WBBB 105, Forschungsstrasse 111, 5232 Villigen PSI, Switzerland.
E-mail addresses: lena.nenoff@psi.ch (L. Nenoff), francesca.albertini@psi.ch (F. Albertini).

https://doi.org/10.1016/j.radonc.2021.03.021
0167-8140/

can bring a benefit to NSCLC patients [13–16]. Nevertheless, the anatomy of these patients is typically changing during the treatment course and the breathing motion makes an irradiation with protons challenging. Motion mitigation techniques such as rescanning [17], gating [13], tracking [18], 4D-optimisation [19,20] or deep-inspiration breath-hold (DIBH) [21] can handle the latter, while for the former fast online daily plan adaption can restore the target coverage [22,23]. Previous studies showed that the dose degradation caused by changing anatomy is more severe than that caused by intra-fractional changes (patients treated in free breathing with rescanning) and makes treatment plan adaption necessary [24].

At PSI an online DAPT workflow has recently been developed [25] and successfully tested for non-deforming anatomies on a phantom [26]. In the DAPT workflow a daily CT is acquired in treatment position, contours are transferred and a plan is reoptimised online [27], followed by a fast clinical and measurement-free physical quality assurance [28]. After the delivery, the dose is reconstructed on the planning CT [29,30]. One of the main requirements to deliver an online adaptive workflow is speed. Ideally the time-span between the acquisition of the daily image and the start of the delivery of the treatment should be comparable to the time-span of the standard delivery. This can only be achieved if no human corrections are done during the process, including no additional correction of the daily structures. Although automatic segmentation decreases the time required for online contour definition, limiting the human correction will inevitably result in daily structures with some residual uncertainties [31]. The impact of such uncertainties on the dose distributions is however still unknown.

In this study, the dosimetric impact of optimizing a daily plan on uncorrected propagated structures is investigated. In particular, we compare the dosimetric effects of *propagated DAPT doses* (optimised with rigidly and DIR propagated structures) to *non-adapted doses* and *ideal DAPT doses* (optimized on structures contoured by a radio-oncologist).

Materials and methods

Patient data and treatment plans

For this retrospective study, a subset of five NSCLC patients with different patient geometries and a complete dataset composed of one planning and nine repeated CTs (three CTS in consecutive DIBHs acquired on day of 2nd, 16th and 31st treatment fraction, respectively) were selected from a dataset of locally advanced NSCLC patients (median age 67 years, range 46–80) treated between 2012 and 2013 with photon therapy [32]. All CTs were acquired in voluntary visually guided DIBH. Although multiple CTs were acquired on the same day, each repeated CT was, for the purpose of this study, considered to represent one independent daily patient anatomy. Structures (gross tumour volume (GTV), clinical target volume (CTV) and relevant OARs) were contoured by the same experienced radiation oncologist on all ten CTs per patient. Intensity modulated proton therapy treatment plans with 60 Gy-RBE (RBE = 1.1) in 2 Gy-RBE per fraction were optimised on a planning target volume (PTV), which was generated by a homogeneous extension of the CTV by 5 mm [33]. Plans consisting of three individually selected fields [24,33–35] were optimised using an in-house developed planning system and analytical dose calculation algorithm [27,36].

Image registrations

The repeated CTs were first rigidly registered to the planning CT with focus on the vertebra using Velocity (Varian Medical Systems, Palo Alto, USA). Then, six different DIRs were applied (two open source Demons and B-splines algorithms [37,38] from Plastimatch and four commercial algorithms one from Velocity [39], one from Mirada (Mirada Medical, Oxford, UK) [40] and two, Anaconda [41] and Morfeus [42], from RayStation (RaySearch Laboratories, Stockholm, Sweden)). All algorithms, except Morfeus, have been used without a focus region. For Morfeus, the lung contours were used as a controlling region of interest. The details about the DIR algorithms used in this study are given in the supplement.

Calculation of DAPT and non-adapted doses

A scheme of the workflow used in this paper is shown in Fig. 1. The planning structures (target and OARs) of all five patients were propagated to the corresponding repeated CTs with rigid registration and with each of the six DIR algorithms using Plastimatch. The PTV for the DAPT plans was generated from each propagated CTV by expanding it by 5 mm, as done for the planning CT. *Propagated DAPT doses* were optimised based on each propagated structure set (*DIR DAPT doses* and *rigid DAPT doses*), *ideal DAPT doses* were optimised based on the reference structures defined by the medical doctor on each repeated CT. This resulted, for each repeated CT, in eight dose distributions optimised on different daily structures. Additionally, a worst-case *non-adapted dose* was generated by recalculating the treatment plan on the repeated CTs.

Evaluation

The *non-adapted, propagated DAPT* and *ideal DAPT doses* were evaluated on each repeated CT using the reference structures defined by the medical doctor. The CTV V95, D2 and the V20 of both lungs excluding GTV of the *non-adapted doses* and the *propagated DAPT doses* were compared to the *ideal DAPT doses* (optimised on the reference structures). Additionally, the structures were reviewed visually, and the overlap (the percentage of the reference structure covered by the propagated structure) of the propagated CTV and the reference CTV evaluated in Matlab (MathWorks, Natic, USA).

Results

As expected, a visual review of the different propagated CTVs showed substantial differences. Fig. 2 shows an example slice of the CTVs propagated with the different algorithms and the reference structure manually contoured on the CT at the end of the treatment. The overlap between the propagated structures with the reference structures (table 1) is on average between 79.1% (patient 2) and 93.8% (patient 4). For example, for patient 1 the CTV shift and shrinkage between the rigid (blue) and the reference structure defined on this CT (green) is not followed completely by the CTVs propagated with the different DIR algorithms. For other patients and other slices of these patients however, all the structures agree.

The dosimetric impact of optimising the plan based on the uncorrected propagated structures is shown in Fig. 3. The differences between CTV V95 and D2 of the *non-adapted doses*, *DIR DAPT doses* and *rigid DAPT doses* to the *ideal DAPT doses* are shown. If the DAPT plan was optimised on the propagated structures with DIR (black), the CTV V95 differed on average by 0.04%, compared to the *ideal DAPT doses*. With the rigid structure propagation (blue) the differences were only slightly larger (0.6%). However, for the *non-adapted doses* (red), the CTV V95 was reduced by an average of 9.7% and the hotspots (e.g. CTV D2) increase severely (up to 12.8% higher for patient 2). DAPT reduced hotspots, independently from the accuracy of the structures used for optimization. For patient 4 larger differences between the *ideal DAPT doses* and the

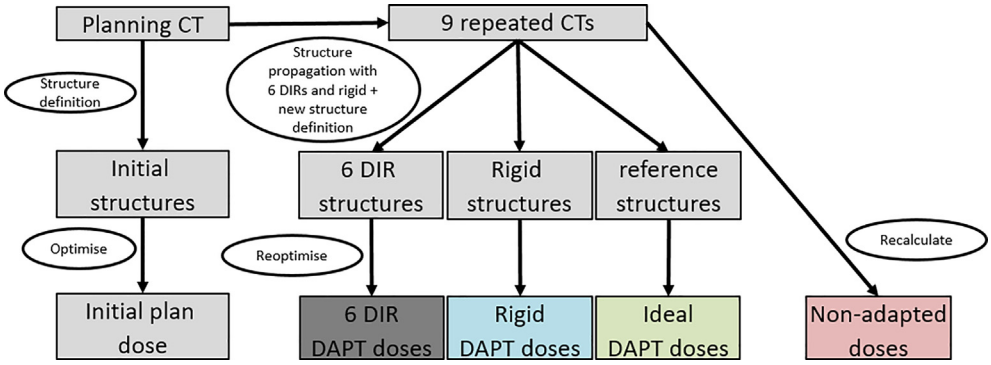

Fig. 1. Scheme of the workflow. On the planning CT, structures and an initial treatment plan was defined for all 5 patients. For each patient, nine repeated CTs were available. The planning structures were transferred to the repeated CTs using 6 different DIRs and a rigid registration. Additionally, new reference structures were defined on each repeated CT by a medical doctor. *Propagated DAPT doses* were re-optimised using the structures propagated rigidly (*rigid DAPT doses*) and with each DIR algorithm (*DIR DAPT doses*). *Ideal DAPT doses* were optimized on the reference structures. *Non-adapted doses* were obtained by recalculating the initial plan on the repeated CTs.

propagated DAPT doses (DIR and rigid) are visible. For this patient lymph nodes have shrunk substantially during the therapy (Fig. 4), which was not completely transformed by the propagated structures. Consequently, the target volume from the reference structure set was smaller than the one from the propagated structures.

The absolute dose to the OARs, for example the V20 of the lung excluding GTV, is mainly depending on the tumour location. The effect of DAPT is however different (Fig. 3c). For some patients with large tumour changes, not adequately represented through the propagated structures, larger difference between the *ideal DAPT doses* and the *propagated DAPT doses* are detected. For example, the V20 of the lung excluding GTV of patient 4 increased in average by 3.3% (*DIR DAPT doses*) or 3.5% (*rigid DAPT doses*) compared to the *ideal DAPT doses*. With a non-adapted approach however, the V20 for this patient would be even higher (5.0% difference compared to the *ideal DAPT dose*). For other patients (e.g. patient 2) using the reference structures for DAPT optimization slightly increased the dose to the lung (up to 2% compared to rigidly propagated structures).

In Fig. 4, the difference between the non-adapted dose, an example of a propagated DAPT dose and the ideal DAPT dose from a CT at the end of treatment is shown. The non-adapted doses show severe hotspots or dose degradations in the target. However, also for the patients with a large target variation (for example patient 1 and 4 in Fig. 4), there is a clear advantage in performing a daily adaptive treatment, instead of using the "worst-case" non-adaptive approach (reduction of hotspots, target coverage for patient 2).

Discussion

In this study, we show that DAPT is beneficial for NSCLC patients treated in DIBH, even if the online daily optimisation is based on uncorrected, propagated structures. The target coverage is only slightly affected (CTV V95 difference <1%) if the daily plan is optimized based on the uncorrected propagated structures compared to the *ideal DAPT plan* (optimised on the structures contoured by a radiation oncologist). If the treatment is not adapted however, the target coverage is reduced (average CTV V95 difference 9.6%) and large hotspots appear (up to 140%), which are always reduced with DAPT (Figs. 3 and 4). For some patients however, DAPT could be beneficial also for specific OARs compared to no adaption and for some OARs a benefit of the *ideal DAPT dose* over *propagated DAPT doses* was seen (Fig. 3c). These results are in line with the findings of Qiao et al. [43], who reported that using automatically segmented structures might facilitate the introduction of online adaptive proton therapy for prostate cancer.

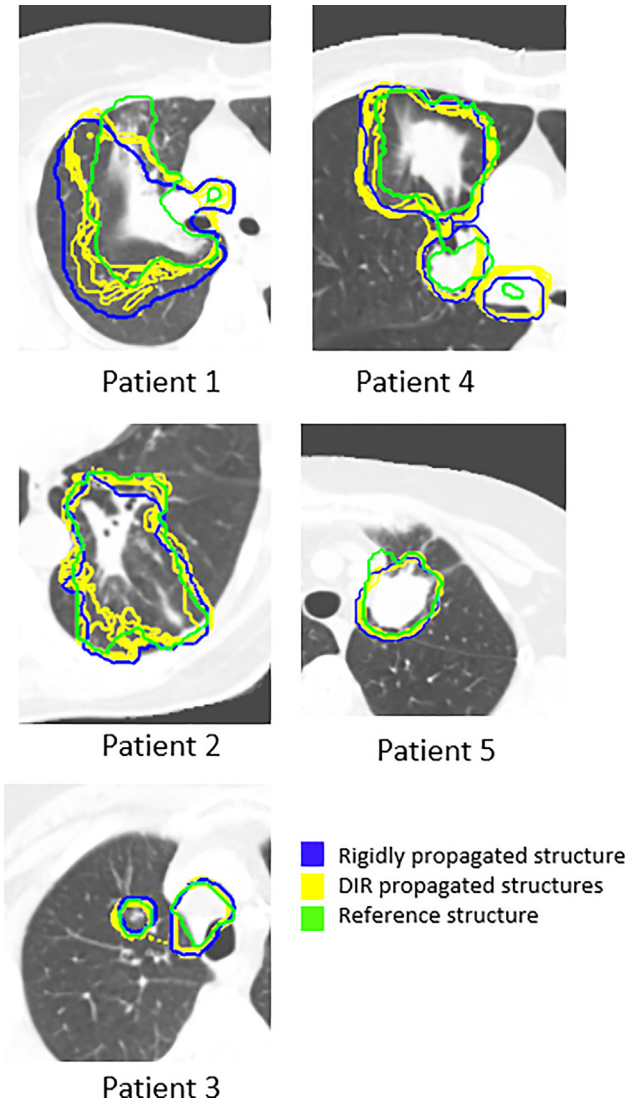

Fig. 2. Examples of the CTV structures propagated rigidly (blue) or by the different DIRs (yellow) and the reference structures defined by a doctor (green) on a repeated CT from the end of the treatment. The structures differ between each other. For example the tumour shrinkage of patient 4 defined by the radiation oncologist is not following the propagated structures.

Table 1
Average and range of the overlap of the propagated CTVs with the reference CTVs of the corresponding repeated CT.

Patient	Average [range] overlap / %
1	89.0 [79.1–94.1]
2	79.1 [66.7–87.4]
3	87.2 [74.8–91.0]
4	93.8 [81.5–97.3]
5	82.0 [33.6–94.1]

It should be noted that the propagated CTVs (either rigidly or with DIR) differ from the reference CTV contoured by the radiation oncologist (Fig. 1, Table 1). This is especially noticeable in case of major tumour changes during the course of therapy (patient 1 and 4, Fig. 2). For these patients, the lymph nodes and the primary GTV shrank during the treatment course. Despite this residual variation in the structure, and independently from the structure propagation method, DAPT showed a dosimetric improvement over a non-adapted treatment.

Interestingly, we found no advantage for the target coverage or OAR doses if the daily plan was optimized based on the deformable instead of rigid contour propagation. For the lung without GTV however, the ideal DAPT plan optimized on the reference structures would be beneficial for some patients. For the cases reported here, the increase of dose to the OARs did not violate any prescribed dose tolerances.

In clinical practice, if large anatomical changes are observed, the plan would be adapted offline. Therefore, the completely non-adapted scenario investigated in this study might overestimate the effects of DAPT compared to a clinical scenario. Therefore, the non-adaptive doses can be seen as a worst case scenario.

For this study, the structures defined by an experienced radiation oncologist were used as reference. Although this is the clinical approach used for offline adaption, it has some limitations. For example, it has been shown that structures defined by different medical doctors [44,45] and even by the same doctor at different times differ between each other [45]. Additionally, the CTV was based on the macroscopic GTV visible in each fraction. However, it is debatable how to properly deal with shrinkage occurring during treatment. Indeed, a shrinkage of the macroscopic tumour volume does not coincide per se with a reduction of the microscopic spread and it is still unclear which is the minimum therapeutic dose that has to be delivered to treat the microscopic spread [46]. The LARTIA Trial reported promising results for adaptive therapy with a reduced CTV for Stage III NSCLC tumour patients with photon therapy [47]. Other studies, instead showed the risk of under-dosing the remaining CTV [48]. Large clinical trials are needed to establish a safe clinical practice of how to deal with tumour shrinkage for NSCLC patients [46,49,50].

It is acknowledged that lung tumours are one of the most challenging indications for proton therapy. Besides intra-fractional motion, the dose calculation in low-density lung tissue has large uncertainties and large inter-fractional changes are expected to occur [24,51–53]. Each of these challenges are discussed separately in the following paragraphs.

Intra-fractional changes can be mitigated through rescanning [17], gating [13], tracking [18], 4D-optimisation [19,20] or DIBH [21]. Visually guided DIBH was the one simulated in this study. We assumed that the entire treatment dose was delivered within one breath-hold. This is however a simplification: the breath can be held in a standard situation for around 20 to 30 seconds [33]. Thus, depending on the tumour size, it might take two to five breath-holds to deliver a field. However, with current developments in controlled breath-hold [54], it is possible to hold the breath up to several minutes. Combined with recent investigations about decreasing delivery times [55], the delivery of the entire field in future will be possible within one breath-hold. Additionally, pre-

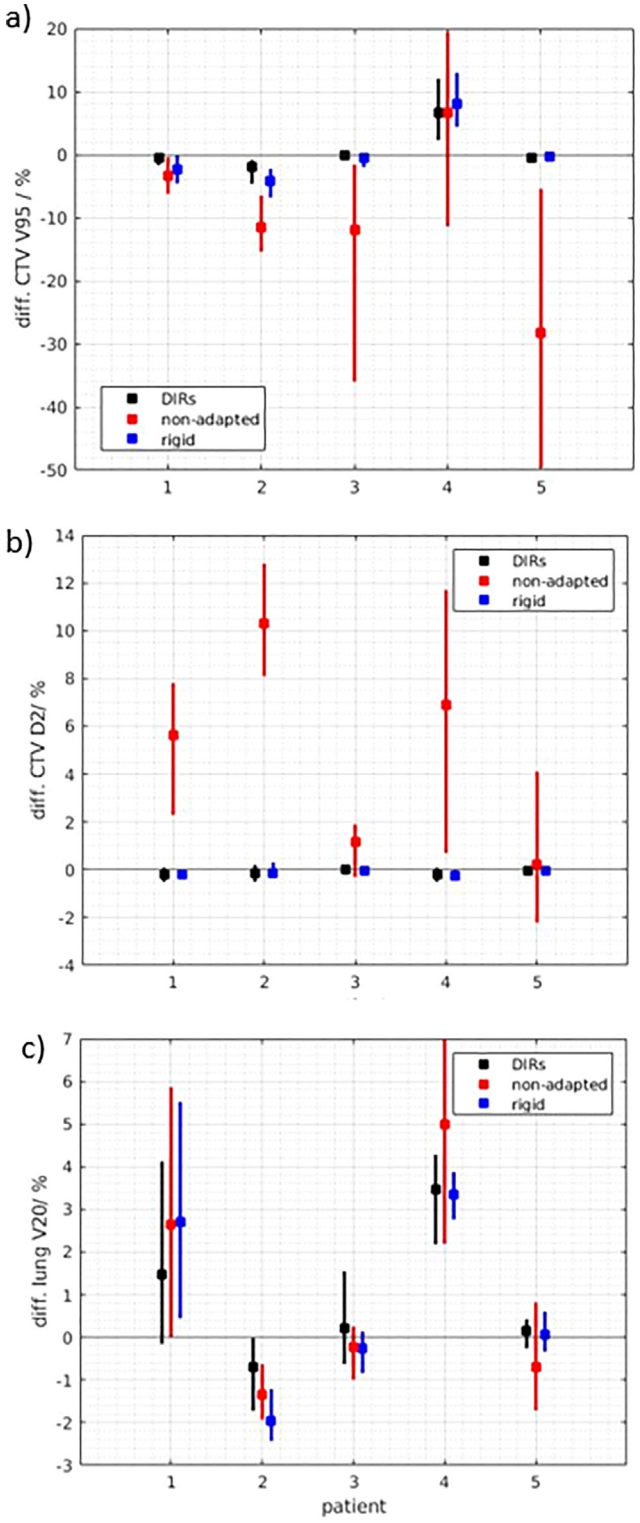

Fig. 3. Differences between the CTV V95 and the CTV D2 and the V20 of the lung without GTV of the ideal DAPT doses, based on the reference structures defined by a radiation oncologist, to the DIR DAPT doses (black), rigid DAPT doses (blue) and non-adapted doses (red). The bars show the range and the box the average difference over all DIRs and fractions. The bars for the rigid (blue) and non-adapted (red) dose parameters contain nine data points (one from each repeated CT), the bar of the DIR (black) dose parameter contains 54 data points (nine CTs times six DIR algorithms per patient).

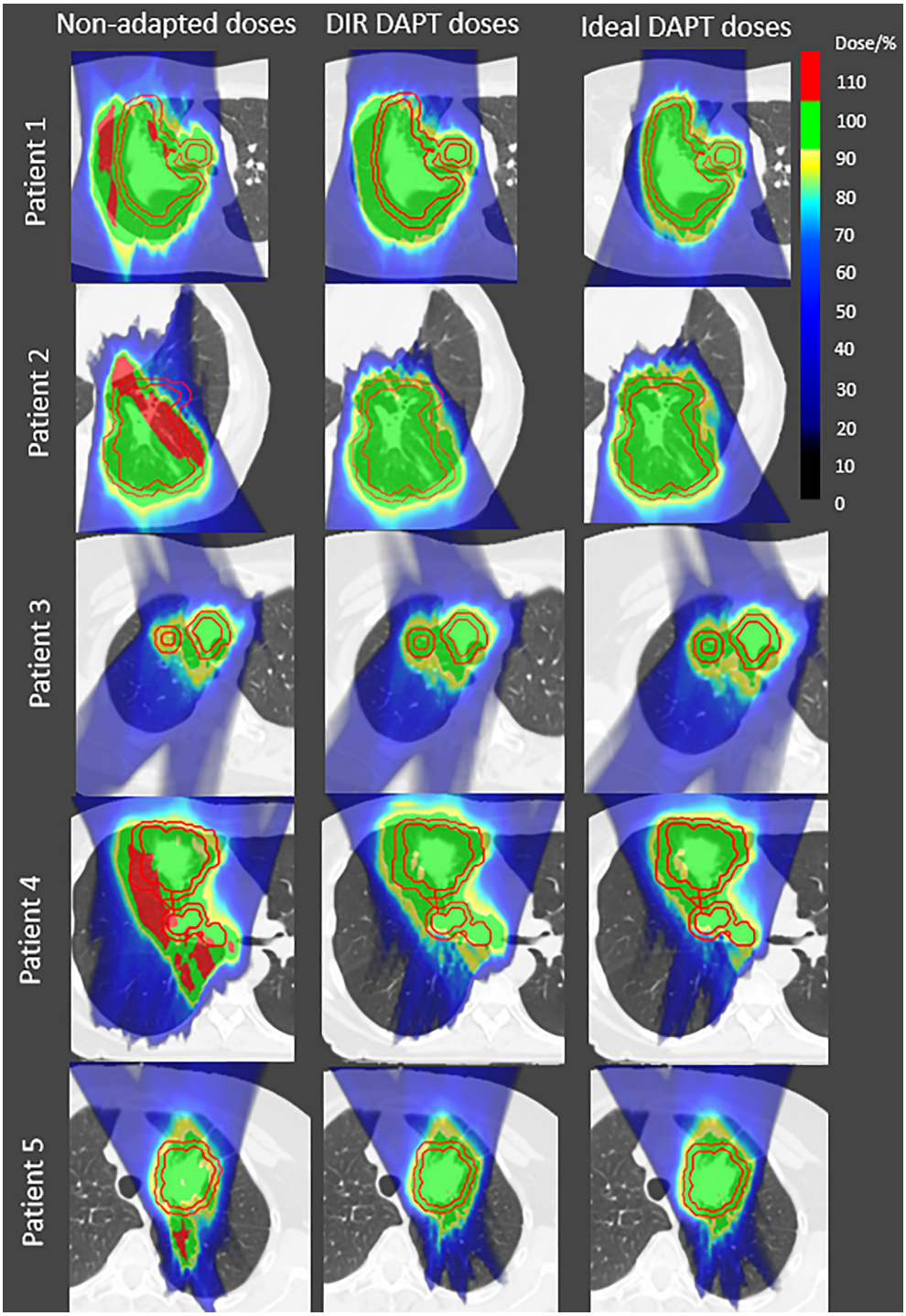

Fig. 4. Example slice of the *non-adapted dose*, *DIR DAPT dose* and the *ideal DAPT dose* of a CT at the end of treatment for all patients. Reference CTV and PTV structures of this CT are shown in red.

vious studies have also shown a high reproducibility of DIBH for NSCLC patients [32,56].

In this study, the dose was optimized with an analytical dose calculation algorithm. In general Monte Carlo (MC) calculations have smaller dose calculation uncertainties, especially in areas with large density heterogeneities [57–60]. However, in online DAPT, time is a critical factor and even with the fastest available proton MC dose calculations [61–64], a full plan optimization takes ~5 min, while analytical algorithms reoptimise the plan within a few seconds [27]. Additionally, the analytical algorithm used in this study has been shown to compare favourably with full Monte Carlo (TOPAS) dose calculations, with 97.7% and 91.9% of all voxels agreeing within 5% and 3% for a variety of indications, including lung [65] and the difference between the different dose calculation algorithms were negligible compared to those caused by anatomical changes [22]. As such, the online dose optimisation will be done with this analytical dose calculation algorithm. The workflow however could be extended with a fast MC dose recalculation before the delivery of the new plan, which could run in parallel to the plan QA and delivery preparation, such that a MC calculated dose would

be available before the delivery of the daily plan. After the delivery, an offline QA with a log-file based MC dose reconstruction would then be performed.

Inter-fractional changes can be addressed with adaption [24]. Because of the large and fast anatomical changes, NSCLC patients might especially benefit from an adaptive workflow. The online daily adaptive strategy followed in this study is similar to the standard workflow, including a daily planning CT, contour propagation, a full reoptimisation and quality assurance of the treatment plan each day. The biggest challenge in such an online DAPT workflow is to have a structure set available on the daily CT, without requiring additional time and resources. Currently, adaptive structures are either propagated with one DIR algorithm, or segmented using an auto-contouring tool. However, due to the intrinsic uncertainties, with both approaches and independently from the used DIR, the resulting daily structure set has to be corrected by a radiation oncologist [9,12,66]. In an online adaptive workflow the time required for manual corrections normally exceeds the time available in a high-throughput treatment. With this study, we showed that such time-intensive online corrections are not always necessary. The benefits of using a DAPT workflow are evident, even if uncorrected, propagated structures are used for optimisation. To ensure a fast online workflow, structure sets could be checked online only for plausibility, before the daily DAPT plan is delivered. After the delivery, however, a careful structure revision and correction are necessary. A full plan reoptimisation used in this study (a new spot placement, constraint optimisation [27,28]) has the advantage that it allows for an improved plan quality in case of favourable anatomy and also works in the case of major anatomical changes, where the simpler approach of restoring the dose on the new anatomy independent from the daily structures [67] might fail. As part of the offline quality assurance after the delivery, the delivered DAPT dose can then be reconstructed from the delivery logfile, using the daily CT and a MC dose calculation [30,68], as in such an online workflow, no patient specific dose measurements are possible. The daily DVHs should then be evaluated with these offline corrected structures. If major differences between the delivered and the desired dose distributions and DVHs are found, these could then be corrected for in a feedback loop during the next fraction, in a similar way to that described by Matter et al [69]. Manually corrected structures can be used as the reference for the next fractions.

The calculated dose differences between non-adapted and DAPT dose could translate into differences in the clinical outcome (tumour control probability/normal tissue complication probability) of the patient. The calculation of treatment outcome based on treatment doses and with changing target structures is not a straight forward process and was not the scope of this study. However, due to the small dose differences between the DAPT doses optimized with different propagated structures the impact of the structure propagation method is expected to be small. It has to be noted that any outcome differences can only be calculated retrospectively, as the dose differences with and without adaption can only be calculated when the anatomical changes during treatment are known (e.g. repeated CTs). Since the anatomical changes are not known beforehand, a prediction of these differences like in the Dutch model-based approach [70,71] is not possible.

For the structure propagation with rigid image registration, the same rigid image registration was used. Even if applying a separate, local rigid registration per propagated structure might improve the rigid contour propagation for some structures (for example the lung or the heart), this was not considered, as applying several image registrations would not be a realistic option in a clinical workflow.

Finally, we would like to point out some limitations of our study. First, only 5 patients were included. With this limited data set we do not quantify the influence of structure propagation for all NSCLC patients. For instance, the selected patients all had large tumours and showed large anatomical changes during treatment, leading to large dose distortions and can thus be considered as worst-case examples. Nevertheless, as the results are consistently showing that the online DAPT is beneficial for such patients even if optimized on uncorrected propagated structures, this indicates that for the online DAPT implementation it might be enough to perform a fast online plausibility check of the propagated structures combined with a careful offline review. If major differences appear (e.g. large target shrinkages), these can be included in an offline adaption, as already done in the current clinical practice. On the other hand, patients with little or no dose distortions due to anatomical changes might not benefit equally from DATP. For these patients the risk of errors in contour propagation has to be re-assessed and other, offline adaptive strategies, where time allows for a correction of propagated structures, might then be more suitable. Second, the nine CTs of these patents were acquired on only 3 days, but in this study they were used as independent fractions. With this study, we did not aim at investigating the difference between inter- and intra- fractional anatomical changes, as this has been done previously [24,32,72]. Instead, we wanted to have as many CTs of different anatomies from the same patients as possible. We acknowledged that for some CTs acquired on the same day, anatomical variations are smaller that if repeated CTs would have been acquired on consecutive days. Nonetheless, repeated CTs from the beginning, mid and end of treatment were included, thus ensuring that the anatomical variability of the entire treatment was represented. Finally, we simulated the patients image guided positioning with focus in the vertebra, with the surrounding anatomy being affected by the breath-hold. Alternative image guided positioning methods with focus on the PTV are often used in clinics [31], if a soft tissue positioning device (e.g. in-room CT or CBCT) is available [33]. For patient 5, we recalculated the dose for each repeated CT with both alignment settings (target- and vertebrae-based) and observed similar dose degradations (e.g. CTV V95). Even if the dose degradation with the rigid registration might be overestimated for some patients, we saw large density changes in the beam path with both methods, and consequently dose differences in the recalculated plans. The DAPT plan will restore daily the initial plan quality, independently from the registration method.

In conclusion, we have shown that for the patients investigated here, an online DAPT workflow is beneficial compared to a non-adapted treatment, even if based on uncorrected propagated structures. Daily manual recontouring on each repeated CT only gives a small additional benefit for some patients and OARs. This suggests that the single DAPT fraction could be optimized based on the uncorrected propagated structures, after performing a daily plausibility check of these propagated contours. A careful offline review of the propagated structure is nonetheless always recommended.

Declaration of Competing Interest

The authors declare that they have no known competing financial interests or personal relationships that could have appeared to influence the work reported in this paper.

Acknowledgements

We acknowledge the SNF (project: 165961) and the ESTRO mobility grant for their support. Also, we kindly acknowledge Djamal Boukerroui for data conversion and the Plastimatch community for their fast support.

Appendix A. Supplementary data

Supplementary data to this article can be found online at https://doi.org/10.1016/j.radonc.2021.03.021.

References

[1] Winkel D, Bol GH, Kiekebosch IH, Van Asselen B, Kroon PS, Jürgenliemk-Schulz IM, et al. Evaluation of Online Plan Adaptation Strategies for the 1.5T MR-linac Based on "First-In-Man" Treatments. Cureus 2018;10:e2431. doi:10.7759/cureus.2431.

[2] Winkel D, Bol GH, Kroon PS, van Asselen B, Hackett SS, Werensteijn-Honingh AM, et al. Adaptive radiotherapy: The Elekta Unity MR-linac concept. Clin Transl Radiat Oncol 2019;18:54–9. https://doi.org/10.1016/j.ctro.2019.04.001.

[3] Acharya S, Fischer-Valuck BW, Kashani R, Parikh P, Yang D, Zhao T, et al. Online magnetic resonance image guided adaptive radiation therapy: first clinical applications radiation oncology. Int J Radiat Oncol Biol Phys 2016;94:394–403. https://doi.org/10.1016/j.ijrobp.2015.10.015.

[4] Rudra S, Jiang N, Rosenberg SA, Olsen JR, Roach MC, Wan L, et al. Using adaptive magnetic resonance image-guided radiation therapy for treatment of inoperable pancreatic cancer. Cancer Med 2019;8:2123–32. https://doi.org/10.1002/cam4.2019.8.issue-510.1002/cam4.2100.

[5] Fischer-Valuck BW, Henke L, Green O, Kashani R, Acharya S, Bradley JD, et al. Two-and-a-half-year clinical experience with the world's first magnetic resonance image guided radiation therapy system. Advancesradonc 2017;2:485–93. https://doi.org/10.1016/j.adro.2017.05.006.

[6] Chamunyonga C, Edwards C, Caldwell P, Rutledge P, Burbery J. The impact of artificial intelligence and machine learning in radiation therapy: considerations for future curriculum enhancement. J Med Imaging Radiat Sci 2020;51:214–20. https://doi.org/10.1016/j.jmir.2020.01.008.

[7] Zhang L, Wang Z, Shi C, Long T, Xu XG. The impact of robustness of deformable image registration on contour propagation and dose accumulation for head and neck adaptive radiotherapy. J Appl Clin Med Phys 2018;19:185–94. https://doi.org/10.1002/acm2.12361.

[8] Brock KK, Mutic S, Mcnutt TR, Li H, Kessler ML. Use of image registration and fusion algorithms and techniques in radiotherapy: Report of the AAPM Radiation Therapy Committee Task Group No. 132. Med Phys 2017;44. doi:10.1002/mp.12256.

[9] Lustberg T, van Soest J, Gooding M, Peressutti D, Aljabar P, van der Stoep J, et al. Clinical evaluation of atlas and deep learning based automatic contouring for lung cancer. Radiother Oncol 2018;126:312–7. https://doi.org/10.1016/j.radonc.2017.11.012.

[10] Delpon G, Escande A, Ruef T, Darréon J, Fontaine J, Noblet C, et al. Comparison of automated atlas-based segmentation software for postoperative prostate cancer radiotherapy. Front Oncol 2016;6. https://doi.org/10.3389/fonc.2016.00178.

[11] Zhang T, Chi Y, Meldolesi E, Yan Di. Automatic delineation of on-line head-and-neck computed tomography images: toward on-line adaptive radiotherapy. Int J Radiat Oncol Biol Phys 2007;68:522–30. https://doi.org/10.1016/j.ijrobp.2007.01.038.

[12] Cardenas CE, Yang J, Anderson BM, Court LE, Brock KB. Advances in Auto-Segmentation. Semin Radiat Oncol 2019;29:185–97. https://doi.org/10.1016/j.semradonc.2019.02.001.

[13] Wink KCJ, Roelofs E, Solberg T, Lin L, Simone CB, Jakobi A, et al. Particle therapy for non-small cell lung tumors: where do we stand? A systematic review of the literature. Front Oncol 2014;4. https://doi.org/10.3389/fonc.2014.00292.

[14] Gomez DR, Li H, Chang JY. Proton therapy for early-stage non-small cell lung cancer (NSCLC). Transl Lung Cancer Res 2018;7:199–204. https://doi.org/10.21037/tlcr10.21037/tlcr.2018.04.12.

[15] Simone CB, Ly D, Dan TD, Ondos J, Ning H, Belard A, et al. Comparison of intensity-modulated radiotherapy, adaptive radiotherapy, proton radiotherapy, and adaptive proton radiotherapy for treatment of locally advanced head and neck cancer. Radiother Oncol 2011;101:376–82. https://doi.org/10.1016/j.radonc.2011.05.028.

[16] Gjyshi O, Liao Z. Proton therapy for locally advanced non-small cell lung cancer. Br J Radiol 2020;93:20190378. https://doi.org/10.1259/bjr.20190378.

[17] Grassberger C, Dowdell S, Sharp G, Paganetti H. Motion mitigation for lung cancer patients treated with active scanning proton therapy. Med Phys 2015;42:2462–9. https://doi.org/10.1118/1.4916662.

[18] Krieger M, Giger A, Jud C, Cattin PC, Salomir RV, Bieri O, et al. Liver-ultrasound based motion model for lung tumour tracking in PBS proton therapy. ICCR Proc 2019.

[19] Boye D, Lomax T, Knopf A. Mapping motion from 4D-MRI to 3D-CT for use in 4D dose calculations: A technical feasibility study. Med Phys 2013;40:061702. https://doi.org/10.1118/1.4801914.

[20] Graeff C. Robustness of 4D-optimized scanned carbon ion beam therapy against interfractional changes in lung cancer. Radiother Oncol 2017;122:387–92. https://doi.org/10.1016/j.radonc.2016.12.017.

[21] Boda-Heggemann J, Knopf A-C, Simeonova-Chergou A, Wertz H, Stieler F, Jahnke A, et al. Deep Inspiration Breath Hold - Based Radiation Therapy: A Clinical Review. Int J Radiat Oncol Biol Phys 2016;94:478–92. https://doi.org/10.1016/j.ijrobp.2015.11.049.

[22] Nenoff L, Matter M, Jarhall AG, Winterhalter C, Gorgisyan J, Josipovic M, et al. Daily adaptive proton therapy: Is it appropriate to use analytical dose calculations for plan adaption?. Int J Radiat Oncol Biol Phys 2020;107:747–55. https://doi.org/10.1016/j.ijrobp.2020.03.036.

[23] Nenoff L, Matter M, Hedlund Lindmar J, Weber DC, Lomax AJ, Albertini F. Daily Adaptive Proton Therapy: the key to use innovative planning approaches for paranasal cancer treatments. Acta Oncol (Madr) 2019;63:. https://doi.org/10.1088/1361-6560/aaba8c085018.

[24] Meijers A, Knopf A-C, Crijns APG, Ubbels JF, Niezink AGH, Langendijk JA, et al. Evaluation of interplay and organ motion effects by means of 4D dose reconstruction and accumulation. Radiother Oncol 2020;150:268–74. https://doi.org/10.1016/j.radonc.2020.07.055.

[25] Albertini F, Matter M, Nenoff L, Zhang Y, Lomax A. Online daily adaptive proton therapy. British Institute of Radiology, 2020: 93(1107). https://doi.org/10.1259/bjr.20190594.

[26] Nenoff L, Matter M, Charmillot M, Krier S, Uher K, Weber DC, Lomax AJ, Albertini F. Experimental validation of daily adaptive proton therapy, submitted to Phys Med Biol.

[27] Matter M, Nenoff L, Meier G, Weber DC, Lomax AJ, Albertini F. Intensity modulated proton therapy plan generation in under ten seconds. Acta Oncol (Madr) 2019;58:1435–9. https://doi.org/10.1080/0284186X.2019.1630753.

[28] Matter M, Nenoff L, Meier G, Weber DC, Lomax AJ, Albertini F. Alternatives to patient specific verification measurements in proton therapy: a comparative experimental study with intentional errors. Phys Med Biol 2018;63:205014. https://doi.org/10.1088/1361-6560/aae2f4.

[29] Winterhalter C. Protons Do Play Dice: Validating, Implementing and Applying Monte Carlo Techniques for Proton Therapy. Diss ETH No 25698 2019.

[30] Winterhalter C, Meier G, Oxley D, Weber DC, Lomax AJ, Safai S. Log file based Monte Carlo calculations for proton pencil beam scanning therapy. Phys Med Biol 2019;64:035014. https://doi.org/10.1088/1361-6560/aaf82d.

[31] Wong J, Fong A, McVicar N, Smith S, Giambattista J, Wells D, et al. Comparing deep learning-based auto-segmentation of organs at risk and clinical target volumes to expert inter-observer variability in radiotherapy planning. Radiother Oncol 2020;144:152–8. https://doi.org/10.1016/j.radonc.2019.10.019.

[32] Josipovic M, Persson GF, Dueck J, Bangsgaard JP, Westman G, Specht L, et al. Geometric uncertainties in voluntary deep inspiration breath hold radiotherapy for locally advanced lung cancer. Radiother Oncol 2016;118:510–4. https://doi.org/10.1016/j.radonc.2015.11.004.

[33] Gorgisyan J, Munck af Rosenschold P, Perrin R, Persson GF, Josipovic M, Belosi MF, et al. Feasibility of pencil beam scanned intensity modulated proton therapy in breath-hold for locally advanced non-small cell lung cancer. Int J Radiat Oncol Biol Phys 2017;99:1121–8. https://doi.org/10.1016/j.ijrobp.2017.08.023.

[34] Nguyen Q-N, Ly NB, Komaki R, Levy LB, Gomez DR, Chang JY, et al. Long-term outcomes after proton therapy, with concurrent chemotherapy, for stage II–III inoperable non-small cell lung cancer. Radiother Oncol 2015;115:367–72. https://doi.org/10.1016/j.radonc.2015.05.014.

[35] Ribeiro CO, Meijers A, Korevaar EW, Muijs CT, Both S, Langendijk JA, et al. Comprehensive 4D robustness evaluation for pencil beam scanned proton plans. Radiother Oncol 2019;136:185–9. https://doi.org/10.1016/j.radonc.2019.03.037.

[36] Schaffner B, Pedroni E, Lomax A. Dose calculation models for proton treatment planning using a dynamic beam delivery system: An attempt to include density heterogeneity effects in the analytical dose calculation. Phys Med Biol 1999;44:27–41. https://doi.org/10.1088/0031-9155/44/1/004.

[37] Unser MA, Aldroubi A, Gerfen CR. A multiresolution image registration procedure using spline pyramids. Math Imaging Wavelet Appl Signal Image Process 1993;2034:160–70. https://doi.org/10.1117/12.162061.

[38] Wang He, Dong L, O'Daniel J, Mohan R, Garden AS, Ang KK, et al. Validation of an accelerated "demons" algorithm for deformable image registration in radiation therapy. Phys Med Biol 2005;50:2887–905. https://doi.org/10.1088/0031-9155/50/12/011.

[39] Kadoya N, Fujita Y, Katsuta Y, Dobashi S, Takeda K, Kishi K, et al. Evaluation of various deformable image registration algorithms for thoracic images. J Radiat Res 2014;55:175–82. https://doi.org/10.1093/jrr/rrt093.

[40] Kessler M, Pouliot J. White paper: Deformable registration: What to ask when assessing the options 2013.

[41] RayStation. Deformable Registration in Raystation (White Paper) 2017.

[42] Velec M, Moseley JL, Svensson S, Hårdemark B, Jaffray DA, Brock KK. Validation of biomechanical deformable image registration in the abdomen, thorax, and pelvis in a commercial radiotherapy treatment planning system. Med Phys 2017;44:3407–17. https://doi.org/10.1002/mp.2017.44.issue-710.1002/mp.12307.

[43] Qiao Y, Jagt T, Hoogeman M, Lelieveldt BPF, Staring M. Evaluation of an open source registration package for automatic contour propagation in online adaptive intensity-modulated proton therapy of prostate cancer. Front Oncol 2019;9:1297. https://doi.org/10.3389/fonc.2019.01297.

[44] Jensen NKG, Mulder D, Lock M, Fisher B, Zener R, Beech B, et al. Dynamic contrast enhanced CT aiding gross tumor volume delineation of liver tumors: an interobserver variability study. Radiother Oncol 2014;111:153–7. https://doi.org/10.1016/j.radonc.2014.01.026.

[45] Louie AV, Rodrigues G, Olsthoorn J, Palma D, Yu E, Yaremko B, et al. Inter-observer and intra-observer reliability for lung cancer target volume delineation in the 4D-CT era. Radiother Oncol 2010;95:166–71. https://doi.org/10.1016/j.radonc.2009.12.028.

[46] Kavanaugh J, Hugo G, Robinson CG, Roach MC. Anatomical adaptation—early clinical evidence of benefit and future needs in lung cancer. Semin Radiat Oncol 2019;29:274–83. https://doi.org/10.1016/j.semradonc.2019.02.009.

[47] Ramella S, Fiore M, Silipigni S, Zappa MC, Jaus M, Alberti AM, et al. Local control and toxicity of adaptive radiotherapy using weekly CT imaging: results from the LARTIA trial in stage III NSCLC. J Thorac Oncol 2017;12:1122–30. https://doi.org/10.1016/j.jtho.2017.03.025.
[48] Hugo GD, Weiss E, Badawi A, Orton M. Localization accuracy of the clinical target volume during image-guided radiotherapy of lung cancer. Int J Radiat Oncol Biol Phys 2011;81:560–7. https://doi.org/10.1016/j.ijrobp.2010.11.032.
[49] Sonke J-J, Aznar M, Rasch C. Adaptive radiotherapy for anatomical changes. Semin Radiat Oncol 2019;29:245–57. https://doi.org/10.1016/j.semradonc.2019.02.007.
[50] Sonke J-J, Belderbos J. Adaptive radiotherapy for lung cancer. Semin Radiat Oncol 2010;20:94–106. https://doi.org/10.1016/j.semradonc.2009.11.003.
[51] Meijers A, Seller OC, Free J, Bondesson D, Seller Oria C, Rabe M, et al. Assessment of range uncertainty in lung-like tissue using a porcine lung phantom and proton radiography. Phys Med Biol 2020;65:155014. https://doi.org/10.1088/1361-6560/ab91db.
[52] den Otter LA, Anakotta RM, Weessies M, Roos CTG, Sijtsema NM, Muijs CT, et al. Investigation of inter-fraction target motion variations in the context of pencil beam scanned proton therapy in non-small cell lung cancer patients. Med Phys 2020;47:3835–44. https://doi.org/10.1002/mp.v47.910.1002/mp.14345.
[53] den Otter LA, Kaza E, Kierkels RGJ, Meijers A, Ubbels FJF, Leach MO, et al. Reproducibility of the lung anatomy under active breathing coordinator control: Dosimetric consequences for scanned proton treatments. Med Phys 2018;45:5525–34. https://doi.org/10.1002/mp.2018.45.issue-1210.1002/mp.13195.
[54] Emert F, Missimer JH, Eichenberger PA, Walser M, Lomax AJ, Weber DC, et al. Enhanced-Deep-Inspiration-Breath-Hold superior to High-Frequency-Percussive-Ventilation for respiratory motion mitigation: a physiology-driven, MRI-guided assessment towards optimized lung cancer treatment with proton therapy. Front. Oncol. 2021. https://doi.org/10.3389/fonc.2021.621350. In press.
[55] van de Water S, Belosi MF, Albertini F, Winterhalter C, Weber DC, Lomax AJ. Shortening delivery times for intensity-modulated proton therapy by reducing the number of proton spots: An experimental verification. Phys Med Biol 2020;65:095008. https://doi.org/10.1088/1361-6560/ab7e7c.
[56] Josipovic M, Aznar MC, Thomsen JB, Scherman J, Damkjaer SMS, Nygård L, et al. Deep inspiration breath hold in locally advanced lung cancer radiotherapy: Validation of intrafractional geometric uncertainties in the INHALE trial. Br J Radiol 2019;92:20190569. https://doi.org/10.1259/bjr.20190569.
[57] Grassberger C, Daartz J, Dowdell S, Ruggieri T, Sharp G, Paganetti H. Quantification of proton dose calculation accuracy in the lung. Int J Radiat Oncol Biol Phys 2014;89:424–30. https://doi.org/10.1016/j.ijrobp.2014.02.023.
[58] Maes D, Saini J, Zeng J, Rengan R, Wong T, Bowen SR. Advanced proton beam dosimetry part II: Monte Carlo vs. pencil beam-based planning for lung cancer. Transl Lung Cancer Res 2018;7:114–21. https://doi.org/10.21037/tlcr10.21037/tlcr.2018.04.04.
[59] Taylor PA, Kry SF, Followill DS. Pencil beam algorithms are unsuitable for proton dose calculations in lung. Int J Radiat Oncol Biol Phys 2017. https://doi.org/10.1016/j.ijrobp.2017.06.003.
[60] Schuemann J, Giantsoudi D, Grassberger C, Moteabbed M, Min CH, Paganetti H. Assessing the clinical impact of approximations in analytical dose calculations for proton therapy. Int J Radiat Oncol Biol Phys 2015;92:1157–64. https://doi.org/10.1016/j.ijrobp.2015.04.006.
[61] Botas P, Kim J, Winey B, Paganetti H. Online adaption approaches for intensity modulated proton therapy for head and neck patients based on cone beam CTs and Monte Carlo simulations. Phys Med Biol 2018;64:015004. https://doi.org/10.1088/1361-6560/aaf30b.
[62] Jia X, Schümann J, Paganetti H, Jiang SB. GPU-based fast Monte Carlo dose calculation for proton therapy. Phys Med Biol 2012;57:7783–97. https://doi.org/10.1088/0031-9155/57/23/7783.
[63] Schiavi A, Senzacqua M, Pioli S, Mairani A, Magro G, Molinelli S, et al. Fred: a GPU-accelerated fast-Monte Carlo code for rapid treatment plan recalculation in ion beam therapy. Phys Med Biol 2017;62:7482–504. https://doi.org/10.1088/1361-6560/aa8134.
[64] Senzacqua M, Schiavi A, Patera V, Pioli S, Battistoni G, Ciocca M, et al. A fast - Monte Carlo toolkit on GPU for treatment plan dose recalculation in proton therapy. J Phys Conf Ser 2017;905:012027. https://doi.org/10.1088/1742-6596/905/1/012027.
[65] Winterhalter C, Zepter S, Shim S, Meier G, Bolsi A, Fredh A, et al. Evaluation of the ray-casting analytical algorithm for pencil beam scanning proton therapy. Phys Med Biol 2019;64:065021. https://doi.org/10.1088/1361-6560/aafe58.
[66] La Macchia M, Fellin F, Amichetti M, Cianchetti M, Gianolini S, Paola V, et al. Systematic evaluation of three different commercial software solutions for automatic segmentation for adaptive therapy in head-and-neck, prostate and pleural cancer. Radiat Oncol 2012;7:160. https://doi.org/10.1186/1748-717X-7-160.
[67] Bernatowicz K, Geets X, Barragan A, Janssens G, Souris K, Sterpin E. Feasibility of online IMPT adaptation using fast, automatic and robust dose restoration. Phys Med Biol 2018;63:085018. https://doi.org/10.1088/1361-6560/aaba8c.
[68] Winterhalter C, Fura E, Tian Y, Aitkenhead A, Bolsi A, Dieterle M, et al. Validating a Monte Carlo approach to absolute dose quality assurance for proton pencil beam scanning. Phys Med Biol 2018;63:175001. https://doi.org/10.1088/1361-6560/aad3ae.
[69] Matter M, Nenoff L, Marc L, Weber DC, Lomax AJ, Albertini F. Update on yesterday's dose-Use of delivery log-files for daily adaptive proton therapy (DAPT). Phys Med Biol 2020;65:195011. https://doi.org/10.1088/1361-6560/ab9f5e.
[70] Langendijk JA, Lambin P, De Ruysscher D, Widder J, Bos M, Verheij M. Selection of patients for radiotherapy with protons aiming at reduction of side effects: The model-based approach. Radiother Oncol 2013;107:267–73. https://doi.org/10.1016/j.radonc.2013.05.007.
[71] Widder J, van der Schaaf A, Lambin P, Marijnen CAM, Pignol J-P, Rasch CR, et al. The quest for evidence for proton therapy: model-based approach and precision medicine. Int J Radiat Oncol Biol Phys 2016;95:30–6. https://doi.org/10.1016/j.ijrobp.2015.10.004.
[72] Meijers A, Jakobi A, Stützer K, Guterres Marmitt G, Both S, Langendijk JA, et al. Log file-based dose reconstruction and accumulation for 4D adaptive pencil beam scanned proton therapy in a clinical treatment planning system: Implementation and proof-of-concept. Med Phys 2019;46:1140–9. https://doi.org/10.1002/mp.13371.